Proceedings World Geothermal Congress 2023
Beijing, China, April 17 – 21, 2023

Numerical analysis on the damage characteristics of hot dry rock subjected to axial-torsional coupled percussion

Zhaowei Sun, Xiaoguang Wu*, Zhongwei Huang, Chao Xiong, Zixiao Xie, Han Chen

Mailing address: State Key Laboratory of Petroleum Resources and Prospecting, China University of Petroleum, Beijing, 102249

E-mail address: cupk2017015165szw@163.com & wuxg@cup.edu.cn (Contact author)

Keywords: Hot dry rock; Percussive drilling; Damage analysis; Thermo-structural analysis

ABSTRACT

Axial-torsional coupled percussive drilling (ATCPD) is a promising method showing merits in creating volumetric breaking patterns and improving drilling rate of hard rocks, and thereby has attracted more and more interest recently in hot dry rock (HDR) geothermal drilling. To determine the dynamic single-cutter-rock interaction behaviors of ATCPD in HDR, we adopted a 3D FEM based thermo-structural coupled modelling approach. In this approach, a damage-viscoplasticity model accounting for the high strain rates was employed to characterize the rock failure. Thermal boundary conditions were implemented by the concrete damage plasticity code. Based on this model, we simulated the cutting process of the single cutter at different percussive modes (axial percussion, torsional percussion, axial-torsional percussion) and analyzed the corresponding damage evolution processes. By conducting the sensitivity analysis, the effects of the temperatures, the dynamic impact loads, and the ratio of the axial impact to torsional impact frequency on the stress around the cutter were investigated. Rock scratch experiments were further conducted on granite specimens under different temperatures to validate the numerical model. The results indicate that the axial and torsional percussion contribute to the generation of rock cohesive and tensile damage, respectively. Unlike them, ATCPD shows more excellent damage performances of HDR, resulting in a 117.73% increase in average Mises stress. This promoting effect can increase the displacement of the cutter in the penetration direction and the cutting direction, so that the excellent ROP enhancement performance in the same rock breaking time is generated by the axial-torsional coupled percussion method. The penetration force and cutting force of the cutter within the same rock breaking depth, as well as the Mise stress inside the rock, decrease with increasing rock temperature, but the trend of forces changing with depth remains unchanged, and higher cutting and penetration displacement are generated in elevated temperature rock. This phenomenon can be validated by the fluctuation of the tensile stress and compressive stress. The larger the axial impact force and the torsional impact torque, the cohesive and tensile damage area will increase at high temperatures. he stress and displacement of coupled percussion rock breaking show significant differences with the change of impact frequency matching in different rock temperatures. That is, the efficiency of geothermal drilling will be influenced by the matching of the rock temperatures and the impact parameters. Our findings are expected to provide an in-depth understanding of percussive drilling mechanisms in HDR.

1. INTRODUCTION

Geothermal energy, as an important clean renewable source of energy, is distinguished by low carbon environmental protection, stability, and efficiency, and includes both hydrothermal and hot dry rock (HDR) geothermal types. At the moment, hydrothermal geothermal energy is the main focus of development. The direct utilization of low and medium temperature geothermal is the first in the world, but HDR geothermal development is still in its early stages. Wang (2012), Li and Wang (2015). HDR is a low-permeability rock mass buried at depths ranging from 3 to 10 km, with the high temperature varies from 150°C to 650°C and little or no water. Pang et al. (2020), Wang et al. (2017) and Gallup (2009). The geologic condition of HDR reservoir is complex, with granites and metamorphic rocks predominating. Some strata rocks have a uniaxial compressive strength of more than 200 MPa, can be drilled up to 10 grades, and have high abrasion resistance. Zeng (2015). This causes serious cutters of bit wear and tear, and the average penetration depth of a single bit is less than 40 m, Li et al. (2022). severely limiting the rate of penetration (ROP) enhancement and making commercial development of HDR energy difficult.

Percussive drilling, as a common mechanical drilling technology in petroleum engineering, has been widely recognized as the most efficient excavation method in hard rock formations. Lundberg and Collet (2010), Wu et al. (2019). Dynamic impact loads and static loads (weight on bit, revolutions per minute, etc.) act on bit, resulting in locally high strain rate rock failure. After drilling, the rock stress distribution includes not only compressive stress but also tensile stress in various directions around the contact region. Thus, the impact stress forces the bit penetrate into the rock, causing various types of cracks, such as radial, intermediate, and side cracks, leading to peel and fracture of rock under the cutters. Tan, Kou and Lindqvist (1998). The application of impact rock breaking to increase ROP is impressive, and rock breaking modes with axial and torsional percussion have been developed. Newman et al. (2009) and Deen et al. (2011). However, the percussive drilling in axial or torsional direction have limitations, whether in terms of bit matching and formation adaptability. The impact energy produced by the axial percussion is relatively small, and excessive impact frequency will also reduce impactor life, so there is no significant advantage in ROP. Suo et al. (2013). Although torsional percussive drilling has a high efficiency of shear rock breaking, it also has a high requirement for the match between the bottom hole assembly when drilling in medium-hard and highly abrasive strata. Tian et al. (2016). As a result, axial-torsional coupled percussive drilling (ATCPD), given full play to the advantages of the axial and torsional percussion, is a promising method showing merits in creating volumetric breaking patterns and improving drilling rate of hard rocks. It is expected to reduce the difficulties associated with hard rock breaking in high temperature-pressure reservoir and thereby has attracted more and more interest recently in HDR geothermal drilling.

In present paper, the rock breaking process of conventional rotary drilling, axial percussive drilling, torsional percussive drilling, and coupled percussive drilling were simulated by applying loads of different degrees of freedom to the cutter in the numerical model, and the rock breaking characteristics under the coupled percussion was obtained by comparative analysis. Furthermore, the temperature of the rock was varied by using coupled percussive drilling as a study subject, and we analyzed the variation laws of the coupled impact rock-breaking properties at different rock temperatures. Finally, the rock was fixed at elevated temperature and the impact parameters on the axial and torsional degrees of freedom were varied to explore the mechanical response properties of the high temperature rocks under different impact parameters matching.

2. NUMERICAL MODEL

During the axial-torsional coupled percussive drilling, the coupled percussion applied to the PDC bit is frequently generated through the impactor, as shown in Fig.1a. The impactor is mounted above the bit. It is propelled by dynamic pressure of the drilling mud. The core structure, including the axial impact hammer and the torsional impact hammer, is assembled and arranged within the tool. The reciprocating impact occurs in the hydraulic drive axial impact hammer. At the same time, the torsional impact hammer has circumferential percussion under dynamic pressure. As a result, two impact energies are combined with static loads (WOB/ torque) to act on the bit cutters, promoting them to penetrate into and cut the rock, as shown in Fig.1b. The rock mechanical properties, static loads, impact parameters, back rake angle, and friction effect at the cutter-rock interface all contribute to the rock-breaking depth and damage stress. We conducted the numerical simulation to solve the complex operation. Figure 1c depicts the plane structure of 3D numerical model. Explicit ABAQUS CAE is utilized for modeling the rock penetration-cutting process. The rock is modelled as a 3D rectangular deformable solid part and the cutter is a discrete rigid element. The bottom and the side part of the rock is fully constrained in all directions while the cutter is free to move in X and Y directions. The diameter of the cutter is 19 mm, the height is 13 mm and the back rake angle is 20°. The geometric dimensioning of the rock model is 75 mm × 150 mm × 150 mm. Both rock and cutter are meshed by the 4-node tetrahedral linear elements(C3D4). Given the accuracy and complexity of the calculation, the mesh on the top of the rock model is refined to ensure better simulation results, and the encrypted mesh size is set to 0.5 mm. Wang et al. (2021) and Yari et al. (2018).

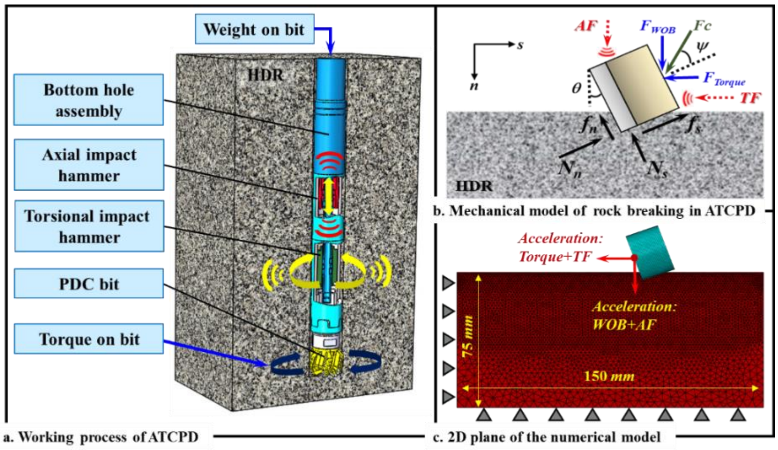

Figure 1: Working process and mechanical-numerical model of ATCPD.

2.1 Rock damage model

The obvious strain rate effect of HDR is occurred with impact dynamic load. The selection of a rock constitutive model should take into account strain rate sensitivity and temperature sensitivity. Furthermore, the chosen model is capable of accurately describing the tensile and compressive deformation characteristics of rock during the percussive drilling. The continuous-discrete coupling algorithm was established in present study. To begin, the concrete damage plasticity (CDP) model in ABAQUS was used to define the material of the rock basic elements. The input material parameters can account for the strain rate effect of rock strength. According to the Zhang, et al. (2022), Genikomsou and Polak (2015)., the yield surface function is defined to characterize rock compressive and tensile equivalent plastic strain in CDP model, which are primarily defined by hardening variables ε_c^{pl} and ε_t^{pl}, respectively. The damage factor is used to describe the stiffness degradation of rock caused by failure, as well as the change in tensile and compressive yield strength. As shown in Fig.2, the failure modes of rock under tension and compression are different. The rock first hardens and then softens after reaching the initial yield stress until crushing failure in the uniaxial compression state. But in the uniaxial tension state, the rock softens after tensile yield until cracking.

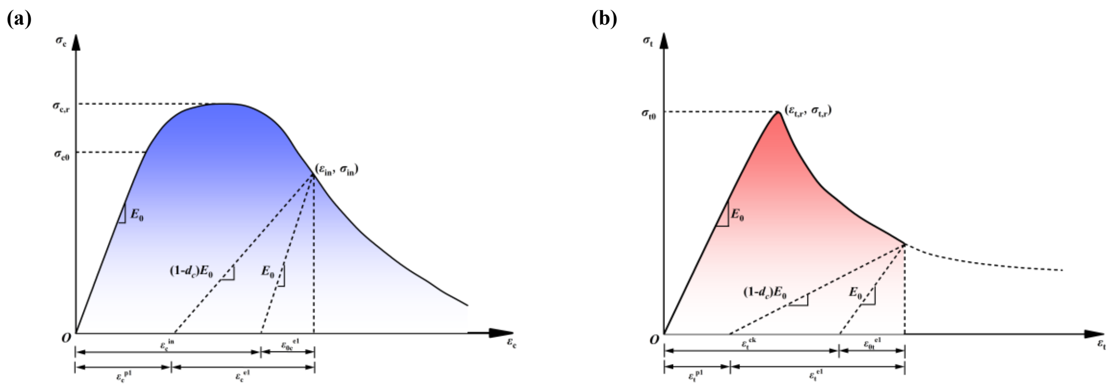

Figure 2: Stress-strain curves of CDP model: a. uniaxial compression; b. uniaxial tension.

To simulate the process of drilling HDR with a PDC cutter, it is necessary to consider how the inherent properties of rock change with temperature. As a result, as shown in Table 1, our model boundary determines the physical parameters of rock at various temperatures. Kuru granite is chosen as the material to simulate hot dry rock in previous studies by Refs. (Song, et al. 2021 and Saksala, et al. 2014). Based on section 2.1, the rock stress-strain curves at different temperatures under tension and compression are predicted in Fig.3, respectively. The damage constitutive curves will be used as temperature domain boundary conditions to perform rock breaking simulations at various temperatures. The information in the curves reveals the failure deformation law of rocks under tensile or compressive stress at different temperatures, and the damage variables calculated supplement the description of rock damage performance at different temperatures and failure modes. It is believed that temperature-dependent rock mechanical properties will have a direct impact on rock breaking, the subsequent mechanism analysis process is detailed.

Table 1: Rock properties for simulations at different temperatures

Rock temperature ℃	Density kg/m^3	Elastic Modulus GPa	Poisson's ratio	Dilation angle °	Shape factor K	Flow stress ratio	Eccentricity	Viscous factor
25	2630	33.66	0.1598	5	0.67	1.16	0.1	1E-05
100	2630	29.66	0.1747	5	0.67	1.16	0.1	1E-05
200	2630	26.24	0.1895	5	0.67	1.16	0.1	1E-05
400	2630	18.63	0.2043	5	0.67	1.16	0.1	1E-05
600	2630	13.14	0.2191	5	0.67	1.16	0.1	1E-05

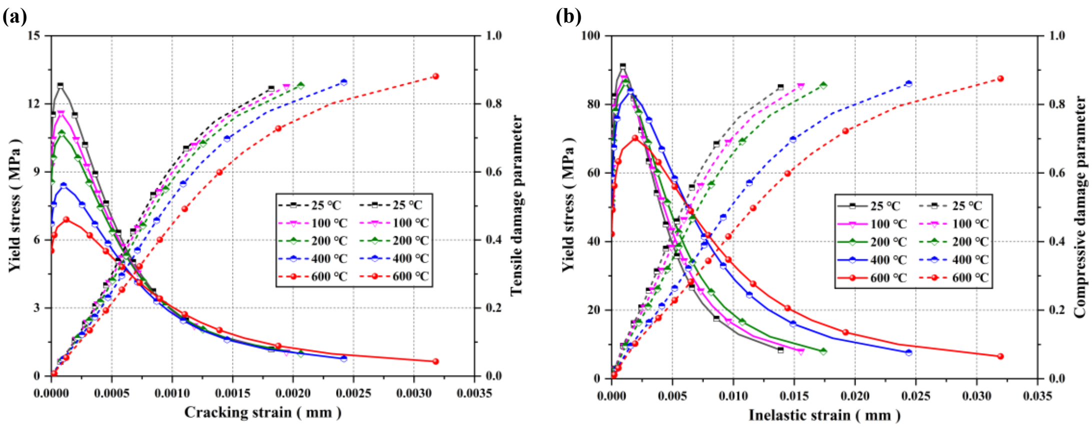

Figure 3: a. The yield stress-cracking strain curves and the damage variable under tension; b. the yield stress-inelastic strain curves and the damage variable under compression.

2.2 Boundary conditions

In the simulation, the single PDC cutter is regarded as rigid body. Elastic Modulus of the cutter is set to 210 GPa. Its Poisson' ratio and density are set to 0.28, 7850 kg/m^3. In order to investigate the rock breaking effect of the axial-torsional coupled percussive drilling, the types of loads applied to the PDC cutter are defined separately. There are two major components, which are as follows: Firstly, static loads (SL) are loads that can be changed on the ground by adjusting pump pressure and RPM, such as WOB, Torque of bit, etc. Secondly, the axial percussion load (APL), torsional percussion load (TPL) and axial torsional coupling percussion load (A-TCPL) generated by the impactor are uniformly defined as dynamic loads. Figure 4a shows the rock breaking diagram of the bit in the above four dynamic-static loads combination methods.

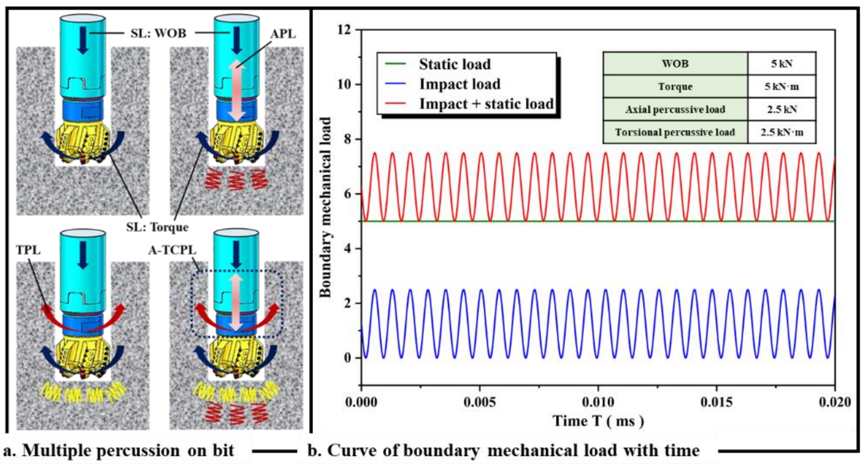

Figure 4: Schematic diagram and mechanical boundary conditions under different percussive modes.

The physical model depicted in Fig.1c is used to investigate the penetration-cutting process of PDC cutter in rock. Except for the cutting and penetration directions, the degrees of freedom of the cutter are completely fixed in all other directions. To explore the process of the bit penetrating the rock, a vertical longitudinal force is applied to the cutter. To simulate the rock breaking process of the PDC cutter, a transverse force is applied along the horizontal direction. Based on the calculation characteristics of the CAE platform explicit dynamics, the calculation time length of up to 500 h if the actual application of drilling rates. According to the research of Cheng, et al. (2018), Majidi, Miska and Tammineni (2011), it was discovered that the rates of PDC cutter has little effect on cutting force and rock breaking characteristics. As a result, in present studies, the cutting and penetration rates are set to 1 m/s (equivalent to applying a force of 5 kN), respectively, in order to effectively reduce calculation time and represent the static loads in two directions, including the WOB and torque. As shown in Fig.4b, the cutter is set to completely drill into the rock for 0.02ms. It is assumed that the cutter is subjected to a sinusoidal continuous impact of the same frequency and an amplitude of 2.5 kN in the axial and torsional directions for 27 times during this time. This dynamic impact loads will be directly applied to the cutter as mechanical boundary conditions of the model to simulate the penetration-cutting process on the rock under different percussive drilling modes.

3. MODEL VALIDATION

Given that the mechanical properties of the simulated rock material are predicted using mathematical methods and that the cutting rates of the cutter differs significantly from the actual, it is necessary to validate the model using experiments. Figure 5 shows experimental equipment and results in our research. The rock scratch test in 25℃ Kuru granite is carried out on a testbed, which is developed on a vertical milling machine, as shown in Fig.5a. The parameters are cutting rates, cutting depth and cutting angle, whose value are set as 5 mm/s, 2 mm and 20 °, respectively. The cutting force is measured and recorded at a 100 Hz sampling rate by load sensor. Simultaneously, the model's vertical degree of freedom is limited to simulate the cutting scratches in the horizontal direction, in which the rock CDP damage constitutive at the same temperature is introduced, and the cutting rate is kept constant at 1 m/s. The quantitative description of the cutting force changes at the bottom of the cutting groove is provided in Fig.5b. The cutting forces obtained by the two methods fluctuate significantly, but due to the influence of rock heterogeneity, the amplitude of the cutting forces obtained by experiment is smaller than the simulation results. The average cutting force calculated by simulation is 3.497 kN, and the average cutting force tested in the laboratory is 3.029 kN, according to statistics. The relative error is maintained at 13.38%. This demonstrates the reliability of our numerical model. The prediction of rock mechanical properties and the application of mechanical loads are consistent with practice.

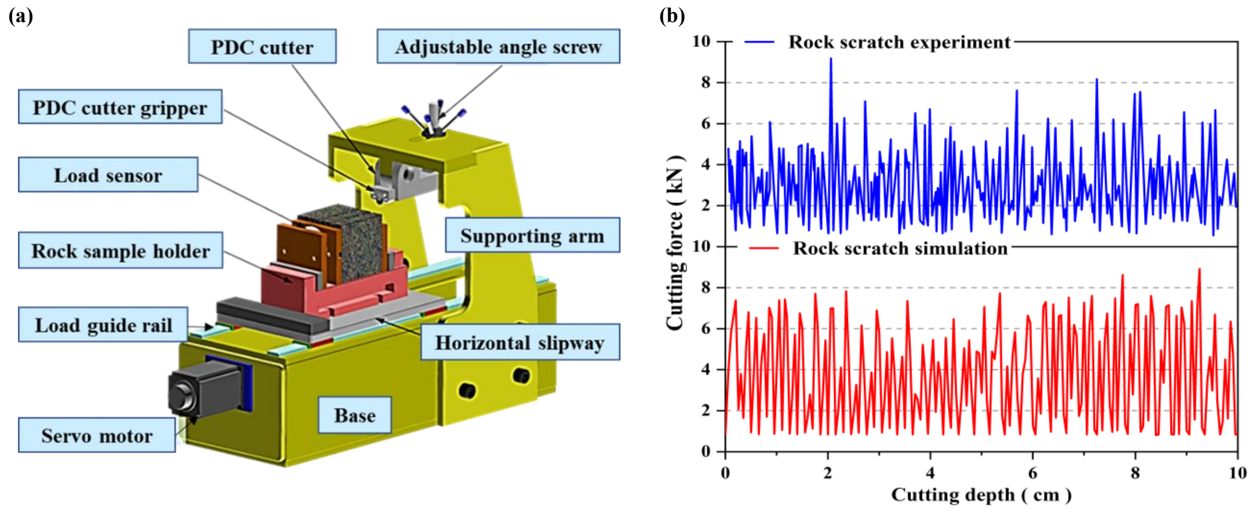

Figure 5: a. Rock scratch test equipment; b. comparison of experimental and simulated cutting forces.

4. RESULTS AND ANALYSES

4.1 Rock-breaking characteristics in ATCPD

The von Mises stress is an equivalent stress that measures the multi-directional stress state of a material and can be used to describe the stress distribution properties. Figure 6 shows the Mises stress distribution of 25 °C rock under four drilling methods at different times. To better analyze the stress distribution of the rocks around the cutter, we unify the stress values at 10.31 ms and 14.81 ms, respectively. Figure shows that the cutter slowly penetrates the rock in the vertical direction and cuts the rock in the horizontal direction under the action of two static loads of WOB and torque. The Mises stress of the rock gradually increases and the stress concentration region first develops in the cutting direction. As the cutter penetrates the rock, the stress under the cutter will gradually increase. However, the application of axial and torsional percussive loads will affect the original stress distribution of this rock. At 10.31 ms, the stress is concentrated in front of the cutter. At the same time, the stress concentration region is also first developed below the cutter during the process of axial percussion. Until 14.81 ms, the stress under the axial percussive drilling is primarily concentrated under the cutter as the rock-breaking progresses, favoring the aggravation of the rock-breaking effect of rock penetration. Compared to rock fracture under static loads, the application of torsional percussive loads significantly increases the stress concentration region in the cutting direction, while the stress distribution below the cutter does not change. This suggests that torsional percussive drilling is beneficial in exacerbating the damage to the rock in the cutting direction. In contrast to the above findings, the rock stress around the cutter under axial-torsional coupled percussion is characterized by both axial and torsional impact rock breaking. Specifically, at 10.31 ms, a larger stress concentration region develops first in the front and under the cutter. This feature does not disappear as the fracture time is extended. When compared to the axial and torsional percussion, the rock stress concentration area developed in the front of the cutter under the coupled percussion at 14.81 ms is similar to the torsional percussion, and the stress concentration area similar to the axial percussion is also retained under the cutter. We predict that the breaking of single cutter by coupled percussion produces stereoscopic damage in both the penetration and cutting directions.

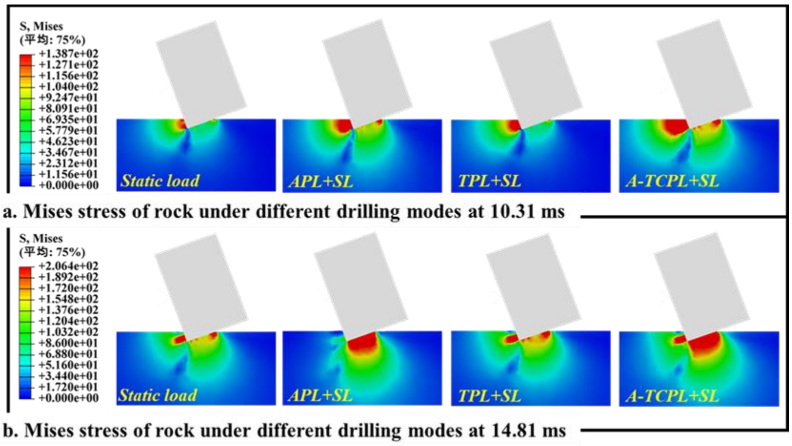

Figure 6: The von Mises stress of rock under different drilling modes: static loads (SL), axial percussive loads (APL) + SL, torsional percussive loads (TPL) + SL, axial-torsional coupled percussive loads (A-TCPL) + SL.

Figure. 7a analyzes the variation of rock stress over time for different drilling methods. As the fracture time of the rock increases, the value of the Mises stress of the rock under the coupled percussion is larger than that of the other drilling modes, and the Mises stress increases linearly and steadily. The average Mises stress under torsional, axial, and coupled percussion gradually increases during the same rock breaking time as the static load case, according to the statistics of the Mises stress during rock breaking. The average Mises stress of the rock increased by 117.73% in the axial-torsion coupled percussive drilling mode. This promoting effect can increase the displacement of the cutter in the penetration direction and the cutting direction, as shown in Figs.7b-c. Compared to conventional rotary drilling, axial percussive drilling, and torsional percussive drilling, the movement displacement of the cutter subjected to the coupled percussion is largest in the cutting and penetration direction. The single cutter is subjected to additional mechanical loading in the cutting direction during stable cutting due to the effect of torsional impact, which increases the amplitude of the cutting force and facilitates high-energy cutting rock fracture. In the penetration direction, negative values of the displacement value indicate the drilling depth of the cutter, and positive values indicate the deformation displacement of the rock elements in front of the cutter during rock breaking. It can be seen that the cut-off under the coupled percussion method obtains a larger penetration depth. At the same time, the degree of deformation of the elements in front of the cutter is also large, yielding the effect of large-scale rock breaking and increased drilling rate.

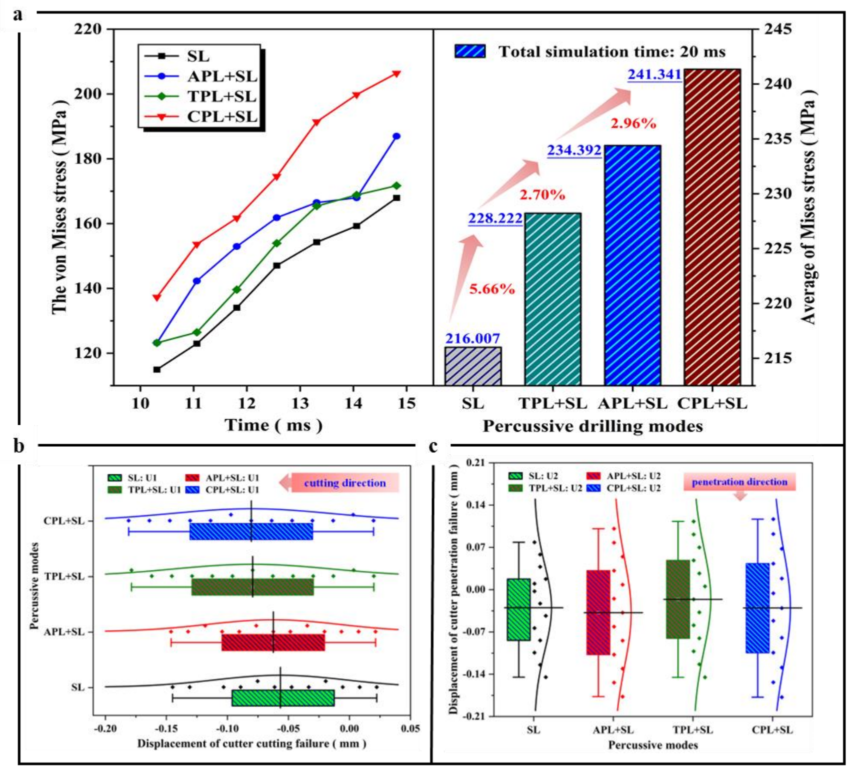

Figure 7: a. The cumulative variation of Mises stress of rock with time; b. the cutting displacement of cutter under different drilling modes; c. the penetration depth of cutter under different drilling modes.

4.2 Failure characteristics of HDR in ATCPD

The properties of hot dry rocks differ significantly from those of normal reservoir rocks. One of the most noticeable characteristics is the rock temperatures. According to the prediction of Figure 3, it can be found that the mechanical response of rock at 600 °C is significantly different from that of rock at 25 °C under tensile or compressive stress. This difference in response is bound to affect rock-breaking properties during bit drilling, but it is not limited to PDC cutter penetration and cutting processes, and the characteristics of high-temperature rock-breaking during percussive drilling are not particularly well understood. We discussed the excellent rock-breaking performance of ATCPD in hard rocks at 25 ℃. In this section, we will use coupled percussive drilling as the sole method and incorporate the rock constitutive quantities set in section 2.1 into the simulation works to investigate the dynamic response characteristics of high-temperature rocks in ATCPD.

Figures 8a-c show the variation of force and stress with rock temperatures for the same displacement of the fixed cutter in the cutting, penetration, and total displacement directions, respectively. The figures show that the rock temperature has no effect on the overall trend of the cutting force and the penetration force of a single cutter with depth. At the onset of rock breaking, the rock is cut and penetrated by the cutter slowly subjected to the coupled percussion, and the rock is pre-broken by 0.045 mm in the cutting and penetration directions, respectively. This phase is distinguished by a rapid agglomeration of cutting and penetration forces that are greater than the rock failure strength to achieve rock breaking. Subsequently, in the cutting direction, the force does not increase as the cutting depth increases, whereas in the penetration direction, the cutter penetrates the rock with a constant slope force. The difference is that a change in the temperature of the rock affects the amplitude of the penetration force and the cutting force of the cutter at the same depth of failure; that is, as the temperature rises, the cutting force and the penetration force decrease in equal proportion. The reason for the disparity is examined in Fig.8c. It is discovered that as the rock temperature rises, the stress produced by breaking the same degree of rock gradually decreases, implying that coupled percussive drilling no longer requires aggregating a larger stress in the HDR to achieve rock breaking. Therefore, the force needed to break HDR at the same depth is decreasing. The displacement of the penetration direction, cutting direction, and resulting force direction are counted in Fig.8d for various rock temperatures over a 20 ms rock breaking period. The failure displacement of the single cutter subjected to the axial-torsional coupled percussion in high temperature rock gradually increases with increasing rock temperature. As a result, we believe that when the cutter outputs the same cutting force and penetration force as when drilling in normal temperature rock, the application of the axial-torsional coupled percussion in hot dry rock can achieve greater failure.

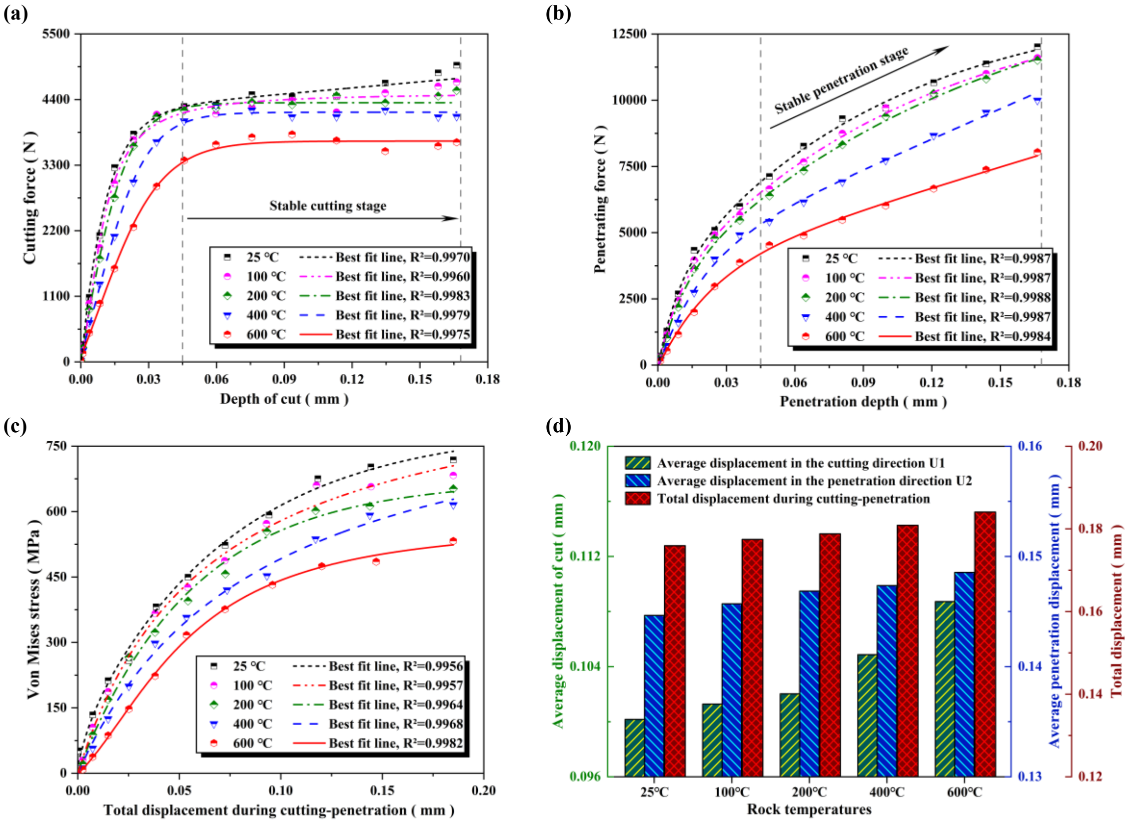

Figure 8: a. Cutting forces at different temperatures in coupled percussion; b. penetration forces at different temperatures in coupled percussion; c. the von Mises stress at different temperatures in axial-torsional coupled percussion; d. the failure displacement of rock varies with rock temperatures

Furthermore, when combined with Fig.3, it can be seen that the ultimate tensile/compressive stress of rock deformation gradually decreases with increasing temperature, indicating that high-temperature rocks are more likely to produce significant tensile and compressive damage. The maximum principal stress of the rock is used as a criterion, with a part above 0 indicating tensile stress and a part below 0 indicating compressive stress. Figure 9 models the tensile and compressive stress profiles in the rock at different temperatures for the same impact parameters and cutter working time. As the rock temperature increases, larger compressive stresses develop below the cutter and more significant crushed zone are predicted. At the periphery of the compressive stress concentration region, a larger tensile stress arc region is generated and a larger tensile-shear damage propagation region is predicted.

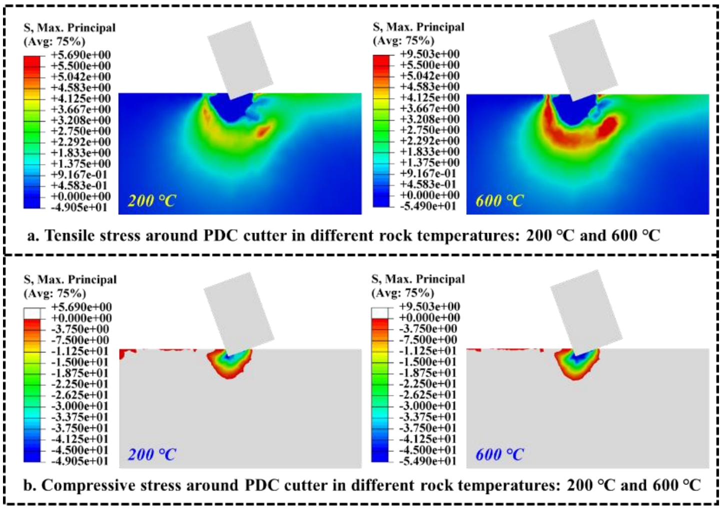

Figure 9: Damage stress around PDC cutter in different rock temperatures

4.3 Effects of the impact amplitude and frequency

4.3.1 The impact amplitude

The matching of impact parameters is the key core of the axial-torsional coupled percussive drilling. This study does not currently take into account the drilling environment of high-temperature rocks. Based on the numerical simulation in Section 4.2, we increase the impact amplitude of 1-4 times in the axial and torsional directions, and discuss the impact parameters matching problem of rock temperature in the range of 200-600 °C. As shown in Fig.10a, the maximum dynamic impact amplitudes in the axial and torsional directions and the static load of 5 kN are increased to 7.5 kN, 10 kN, 12.5 kN and 15 kN, respectively. Figure 10b collects data on rock tensile/ compressive stress when the impact amplitude is only increased in the axial or torsional direction. It can be observed quantitatively and intuitively that increasing the torsional impact amplitude favors the rock to obtain a larger tensile and compressive stress compared to increasing the axial impact amplitude. This is determined by the characteristics of the axial-torsional coupled percussive drilling. Actually, axial percussion primarily assists the PDC bit in increasing its rate in the penetration direction, whereas torsional percussion can assist the bit in increasing the energy of cutting rock breaking on the one hand, and torsional vibration is beneficial in slowing down torque accumulation on the cutters on the other. Mu et al. (2022). As a result, increasing the torsional impact amplitude has a greater ROP enhancing effect than increasing the axial impact amplitude, and this feature is applicable to rocks with temperatures ranging from 200 to 600 °C. It should also be noted that we fitted the tensile and compressive stress data points and discovered that the changes in tensile and compressive stress data under different rock temperatures follow the same mathematical law, indicating that changing the rock temperature has no effect on the damage stress distribution under different impact amplitude ratios. The value of the rock stress increases proportionally to the increase of the rock temperature. Thus, in the study of axial and torsional impact amplitude matching for high-temperature rocks, we believe that the main factor inducing efficient rock failure is the impact amplitude.

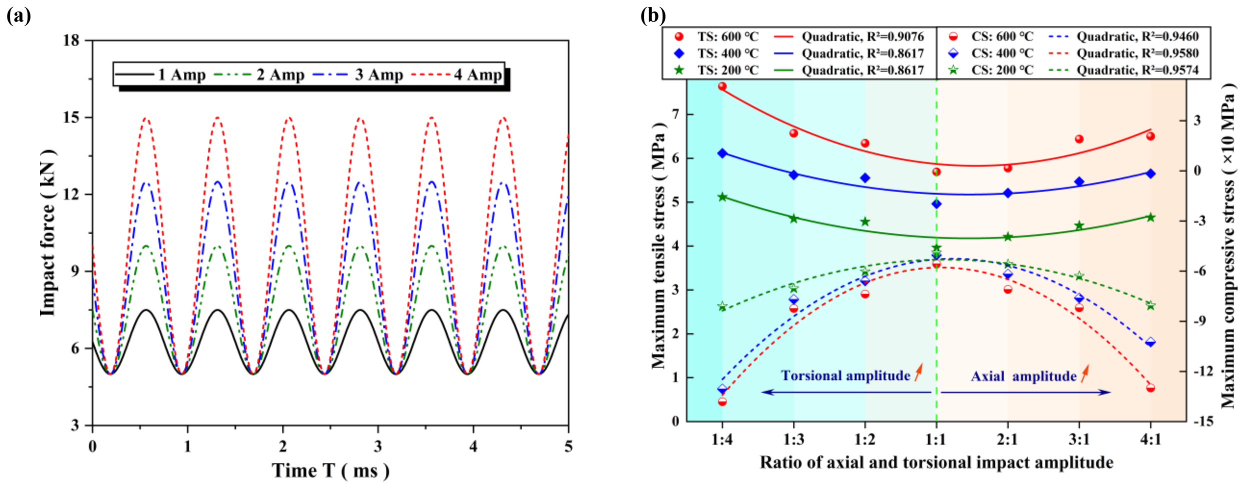

Figure 10: a. Axial/ torsional boundary conditions: the impact force; b. the maximum damage stress varies with ratio of axial and torsional impact amplitude.

4.3.2 The impact frequency

The impact frequency, that is, the number of times the underlying rock is impacted over a period of time, is one of the key parameters of the axial-torsion coupled percussive drilling system. The rock temperature is still dominated by 200 °C, 400 °C, and 600 °C, according to the research conclusions in Section 4.3.1. For the boundary conditions of the PDC cutter, four times of the axial and torsional impact amplitudes are set, and the frequencies of the axial impact force is adjusted to 1/3, 1/2, 2/1 and 3/1 of the original frequency, respectively. Figure 11b depicts the variation of the Mises stress and total displacement for rock breaking at different temperatures for matched axial and torsional impact frequencies. It is found that under different rock temperatures, the stress and displacement of axial-torsional coupling impact rock breaking show significant differences with the change of impact frequency matching, which indicates that rock temperature and impact frequency affect the rock breaking effect together. The optimal values of the axial and torsional impact frequencies do not remain constant across rocks of varying temperatures. We attempt to create an axial and torsional impact frequency matching scheme for high-temperature rock fragmentation. We believe that a ratio of impact frequencies greater than these two values is optimal for efficient rock breaking because the maximum stress and failure displacement of a rock occurs when the axial and torsional impact frequencies are 1:1. According to this theoretical foundation, we find that increasing the axial impact frequency is beneficial for rocks at 200 and 400 °C in order to obtain a larger failure displacement and produce a larger rock stress. When the rock temperature reaches 600 °C, the axial impact frequency is reduced by 1 / 2 of the original, and a better rock breaking effect will be obtained. The behavior of the impact frequency matching method as a function of temperature disorder deserves further exploration.

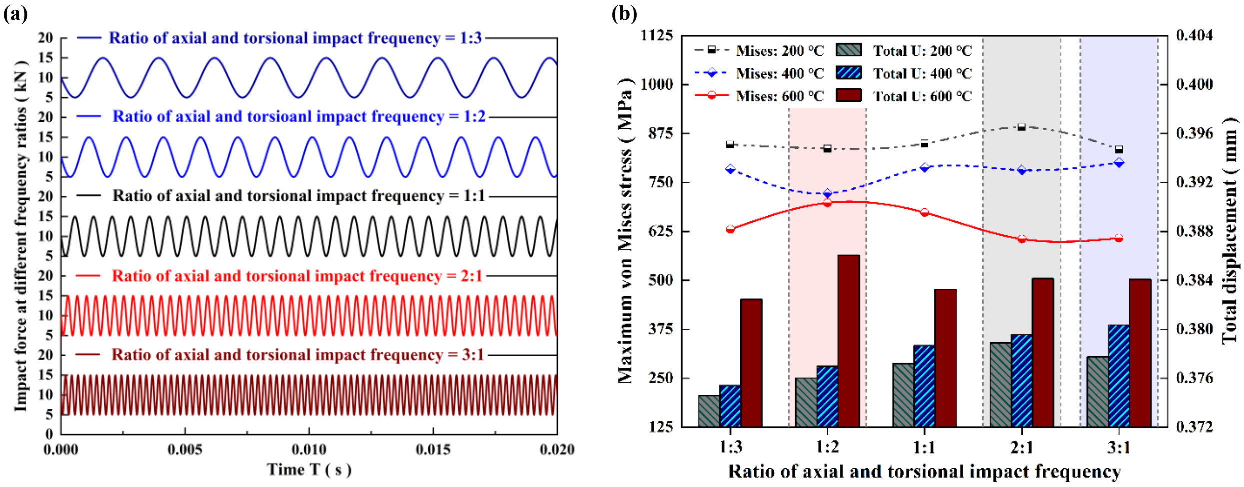

Figure 11: a. Axial/ torsional boundary conditions: the impact frequency; b. the maximum Mises stress and the cumulative displacement varies with ratio of axial and torsional impact frequncy.

5. CONCLUSIONS

To determine the dynamic cutter-rock interaction behaviors of axial-torsional coupled percussive drilling in HDR, a numerical modelling approach describing rock breaking subjected to the axial-torsional coupled percussion with single cutter is established. Compared with conventional rotary drilling, axial percussive drilling, and torsional percussive drilling, the ROP enhancement performance of coupled percussion is illustrated in terms of rock stress, fracture properties, and torque reduction effects. The rock breaking characteristics of axial-torsional coupled percussion in rocks at different temperatures (25 °C -600 °C) are analyzed, and the feasibility of this rock breaking method to achieve drilling rate increase in high temperature rocks is evaluated. Based on the above analysis, the matching principle of axial and torsional impact parameters (amplitude and frequency) for efficient failure of high temperature rock is discussed. The main conclusions are listed as below:

- Applying the axial-torsional coupled percussive rock breaking method, the stress characteristics inside the rock combine the distribution characteristics of axial percussion and torsional percussion, and the stress concentration areas are developed, resulting in a 117.73% increase in average Mises stress. This promoting effect can increase the displacement of the cutter in the penetration direction and the cutting direction, respectively, so that the excellent ROP enhancement performance in the same rock breaking time is generated by the axial-torsional coupled percussion method.

- The rock breaking characteristics of axial-torsional coupled percussion differ in high- and room-temperature rock. The penetration force and cutting force of the cutter within the same rock breaking depth, as well as the Mise stress inside the rock, decrease with increasing rock temperature, but the trend of forces changing with depth remains unchanged, and higher cutting and penetration displacement are generated in high temperature rock. This is caused by a change in the mechanical properties of the rock itself under high temperature conditions. That is, with the same impact parameters, the tensile and compressive damage stress of high temperature rock around the cutter increase, predicting that the rock will fragment on a large scale.

- When the rock temperature range is 200-600 °C, increasing the axial and torsional impact amplitude simultaneously favors the formation of a large damage stress inside the rock. Among them, increasing the torsional impact amplitude can promote a rapid increase of the stress for certain rock temperatures, and that this promotion is better than increasing the axial impact amplitude. Axial-torsion coupled percussive drilling will be applied to hot dry rocks, and efficient rock-breaking effects require impact frequency matching and optimization as well. The stress and displacement of coupled percussion rock breaking show significant differences with the change of impact frequency matching in different rock temperatures, which indicates that rock temperature and impact frequency affect the rock breaking effect together.

AUTHOR STATEMENT

Xiaoguang Wu and Zhongwei Huang conceived the idea for this manuscript. Zhaowei Sun built the model and conducted the numerical simulation. Chao Xiong, Zixiao Xie and Han Chen performed model validation. All authors discussed the results and contributed to the final manuscript.

ACKNOWLEDGEMENTS

The authors give thanks to the financial support of Major Program of National Natural Science Foundation of China (Grant No. 52192624).

REFERENCES

Wang Jiyang. Geothermal energy development under the energy and environmental crisis, *Science and Technology Review*, 2012, 30(04): 3.

Li Dewei and Wang Yanxin. Major issues of research and development of hot dry rock geothermal energy, *Earth Science - Journal of China University of Geosciences*, 2015, 40(11):1858-1869.

Pang Zhonghe, Luo Ji, Cheng Yuanzhi, et al. Evaluation of geological conditions for the development of deep geothermal energy in China. *Earth Science Frontiers*, 2020, 27(1): 134-151.

Wang Guiling, Zhang Wei, Liang Jiyun, et al. Institute of Hydrogeology and Environmental Geology, *Chinese Academy of Geological Sciences*, 2017, 38(04): 449-450+134+451-459.

Gallup D L. Production engineering in geothermal technology: a review. *Geothermics*, 2009, 38(3): 326-334.

Zeng Yijin. Technical progress and thinking for development of hot dry rock (HDR) geothermal resources, *Petroleum Drilling Techniques*, 2015, 43(02): 1-7.

Li Gensheng, Wu Xiaoguang, Song Xianzhi, et al. Status and challenges of hot dry rock geothermal resource exploitation, *Petroleum Science Bulletin*, 2022, 7(03): 343-364.

Lundberg B, Collet P. Optimal wave with respect to efficiency in percussive drilling with integral drill steel, *International Journal of Impact Engineering*, 2010, 37(8): 901-906.

Wu X, Huang Z, Cheng Z, et al. Effects of cyclic heating and LN2-cooling on the physical and mechanical properties of granite, *Applied Thermal Engineering*, 2019, 156: 99-110.

Tan X C, Kou S Q, Lindqvist P A. Application of the DDM and fracture mechanics model on the simulation of rock breakage by mechanical tools, *Engineering Geology*, 1998, 49(3-4): 277-284.

Newman K, Burnett T, Pursell J, et al. Modeling the affect of a downhole vibrator, *Proceedings*, the 2009 SPE/ICoTA Coiled Tubing and Well Intervention Conference and Exhibition, Woodlands, Texas, USA (2009).

Deen A, Wedel R, Nayan A, et al. Application of a torsional impact hammer to improve drilling efficiency, *Proceedings*, the SPE Annual Technical Conference and Exhibition, Denver, Colorado, USA, (2011).

Suo Zhongwei, Wang Jiachang, Zhang Haiping, et al. Application of rotary percussion drilling on the super deep section in Tahe Field, *Oil Drilling & Production Technology*, 2013, 35(04): 44-46.

Tian Jialin, Zhu Yonghao, Wu Chunming, et al. Kinetic characteristic research of a new torque oscillator, *Machinery Design & Manufacture*, 2016, No. 301(03): 75-78.

Wang W, Liu G, Li J, et al. Numerical investigation on rock‐breaking mechanism and cutting temperature of compound percussive drilling with a single PDC cutter, *Energy Science & Engineering*, 2021, 9(12): 2364-2379.

Yari N, Kapitaniak M, Vaziri V, et al. Calibrated FEM modelling of rock cutting with PDC cutter, *Proceedings*, the MATEC web of conferences, 2018.

Zhang Yongjie, Chen Li, Xie Puchu, et al. Rate correlation of the ABAQUS damage parameter in the concrete damage plasticity model and its realization method, *Explosion and Shock Waves*, 2022, 42(10): 39-49.

Genikomsou A S, Polak M A. Finite element analysis of punching shear of concrete slabs using damaged plasticity model in ABAQUS, *Engineering structures*, 2015, 98: 38-48.

Song H, Shi H, Li G, et al. Numerical simulation of the energy transfer efficiency and rock damage in axial-torsional coupled percussive drilling, *Journal of Petroleum Science and Engineering*, 2021, 196: 107675.

Saksala T, Gomon D, Hokka M, et al. Numerical and experimental study of percussive drilling with a triple-button bit on Kuru granite, *International Journal of Impact Engineering*, 2014, 72: 56-66.

Cheng Z, Sheng M, Li G, et al. Imaging the formation process of cuttings: characteristics of cuttings and mechanical specific energy in single PDC cutter tests, *Journal of Petroleum Science and Engineering*, 2018, 171: 854-862.

Majidi R, Miska S Z, Tammineni S. PDC single cutter: the effects of depth of cut and RPM under simulated borehole conditions, *Wiertnictwo, Nafta, Gaz*, 2011, 28(1-2): 283-295.

Mu Z, Huang Z, Sun Z, et al. Experimental study on dynamic characteristics of axial-torsional coupled percussive drilling, *Journal of Petroleum Science and Engineering*, 2022, 219: 111094.